THE JOURNAL OF BIOLOGICAL CHEMISTRY VOL. 283, NO. 32, pp. 22295–22303, August 8, 2008

NFATc2 Is a Necessary Mediator of Calcineurin-dependent Cardiac Hypertrophy and Heart Failure*[S]

Received for publication, February 19, 2008, and in revised form, May 1, 2008 Published, JBC Papers in Press, May 12, 2008, DOI 10.1074/jbc.M801296200

Meriem Bourajjaj[‡], Anne-Sophie Armand[‡], Paula A. da Costa Martins[‡], Bart Weijts[‡], Roel van der Nagel[‡], Sylvia Heeneman[§], Xander H. Wehrens[¶], and Leon J. De Windt[‡‖1]

From the [‡]Hubrecht Institute and Interuniversity Cardiology Institute Netherlands, Royal Netherlands Academy of Sciences, Uppsalalaan 8, 3584 CT Utrecht, The Netherlands, the [§]Department of Pathology, University Hospital Maastricht, P. Debyelaan 25, 6229 HX, Maastricht, The Netherlands, [¶]Baylor College of Medicine, Houston, Texas 77030, and the [‖]Department of Medical Physiology, University Medical Center Utrecht, Yalalaan 50, 3584 CM, Utrecht, The Netherlands

One major intracellular signaling pathway involved in heart failure employs the phosphatase calcineurin and its downstream transcriptional effector nuclear factor of activated T-cells (NFAT). *In vivo* evidence for the involvement of NFAT factors in heart failure development is still ill defined. Here we reveal that *nfatc2* transcripts outnumber those from other *nfat* genes in the unstimulated heart by severalfold. Transgenic mice with activated calcineurin in the postnatal myocardium crossbred with *nfatc2*-null mice revealed a significant abrogation of calcineurin-provoked cardiac growth, indicating that NFATc2 plays an important role downstream of calcineurin and validates the original hypothesis that calcineurin mediates myocyte hypertrophy through activation of NFAT transcription factors. In the absence of NFATc2, a clear protection against the geometrical, functional, and molecular deterioration of the myocardium following biomechanical stress was also evident. In contrast, physiological cardiac enlargement in response to voluntary exercise training was not affected in *nfatc2*-null mice. Combined, these results reveal a major role for the NFATc2 transcription factor in pathological cardiac remodeling and heart failure.

Heart failure, or the inability of the heart to meet hemodynamic demands, represents the end stage of various forms of cardiac disease. In the Western world, the prevalence and incidence of heart failure are increasing steadily, and heart failure is now the leading cause of hospitalization in the elderly. The leading cause of heart failure is left ventricular hypertrophy, defined as an increase in heart size without a change in myocyte number, because chronically hypertrophied hearts remodel and dilate (1, 2). Conversely, not all forms of cardiac hypertrophy are necessarily pathological, as athletic conditioning can stimulate heart growth without deleterious consequences (3). Hence, a better understanding of the mechanisms underlying pathological *versus* adaptive hypertrophic growth of the myocardium is key to develop preventative measures and therapeutics for heart failure patients (4).

Gain- and loss-of-function studies in genetically altered mice and cultured cardiomyocytes have demonstrated the sufficiency and necessity of calcineurin to regulate pathological cardiac hypertrophy (5–12). In contrast, *in vivo* confirmation about the involvement of its direct downstream transcriptional effectors in the heart is still incompletely resolved. Calcineurin dephosphorylates members of the nuclear factor of activated T cells (NFAT)[2] transcription factor family (13), allowing NFAT to translocate to the nucleus where it cooperates with other transcription factors to regulate calcineurin-responsive target genes. The ventricular cardiomyocyte contains all four calcineurin-sensitive NFATc isoforms, NFATc1 (NFATc), NFATc2 (NFATp), NFATc3 (NFAT4), and NFATc4 (NFAT3) (14, 15), and expression of dominant-negative forms of NFAT virtually abolishes calcineurin-mediated hypertrophy in cultured cardiomyocytes (14, 16). *In vivo*, however, *nfatc4*-null mice harboring a cardiac specific calcineurin transgene did not display a compromise of cardiac hypertrophy and heart failure (15). *nfatc3*-null mice are only very partially deficient in their ability to undergo cardiac hypertrophy and display no improvement on hypertrophic marker gene expression or cardiac dysfunction in response to calcineurin activation (15). Combined, a vast disparity exists between *in vivo* and *in vitro* studies concerning the involvement of NFAT factors in cardiac hypertrophy.

Here we provide evidence that NFATc2 mRNA levels are the most abundantly expressed in the heart among all NFAT isoforms. In line, *nfatc2*-deficient mice harboring a calcineurin transgene or subjected to pressure overload are substantially compromised in their ability to undergo cardiac hypertrophy. Moreover, at 8 weeks after pressure overload, echocardiography indicated marked left ventricular dilation and loss of systolic function in wild-type mice, whereas *nfatc2*-null mice displayed a prominent reduction in myofiber hypertrophy, preservation of left ventricular geometry and contractility,

* This work was supported by Grants 912-04-054, 912-04-017, and VIDI Award 917-86-372 from the Netherlands Organization for Health Research and Development and by European Union Contract LSHM-CT-2005-018833/EUGeneHeart (to L. J. D. W.). The costs of publication of this article were defrayed in part by the payment of page charges. This article must therefore be hereby marked "*advertisement*" in accordance with 18 U.S.C. Section 1734 solely to indicate this fact.

[S] The on-line version of this article (available at http://www.jbc.org) contains supplemental methods and figure.

[1] To whom correspondence should be addressed: Dept. of Medical Physiology, Division Heart and Lungs, University Medical Center Utrecht, Yalelaan 50, 3584 CM Utrecht, The Netherlands. Tel.: 31-30-253-8905; Fax: 31-30-253-9036; E-mail: L.J.deWindt@umcutrecht.nl.

[2] The abbreviations used are: NFAT, nuclear factor of activated T-cell; RT, reverse transcription; MHC, myosin heavy chain; WGA, wheat germ agglutinin; LVID, left ventricular internal diameter; FS, fractional shortening; BW, body weight; HW, heart weight; TAC, transverse aortic.

reduced fibrosis, and a diminished hypertrophic gene program. Remarkably, *nfatc2*-null mice were not compromised in their ability to undergo athletic cardiac enlargement. Taken together, these findings reveal a main role for NFATc2 downstream of calcineurin signaling in pathological cardiac remodeling.

EXPERIMENTAL PROCEDURES

Mice—αMHC-calcineurin transgenic mice, described previously (5) and generously provided by Eric N. Olson, were crossbred with mice harboring a *nfatc2* null mutation (17) and generously provided by Laurie Glimcher.

Aortic Banding and Angiotensin II Infusions—Angiotensin II infusion with Alzet 2002 mini isosmotic pumps was performed as described previously (8). Transverse aortic (TAC) banding or sham surgery was performed in *nfatc2*$^{+/+}$ or *nfatc2*$^{-/-}$ mice. The aorta was subjected to a defined, 27-gauge constriction between the first and second truncus of the aortic arch as described in detail previously (18). Pressure gradients between the proximal and distal sites of the transverse aortic constriction were determined by Doppler echocardiography (19) or invasive pressure measurements (18).

Transthoracic Echocardiography—Cardiac remodeling and function were serially assessed at 2, 4, 6, and 8 weeks after TAC surgery by noninvasive echocardiography using a Hewlett-Packard Sonos 5500 instrument (Hewlett-Packard), 15-MHz transducer (15-6L linear probe, Philips Medical Systems) as described in detail previously (19).

Immunolabeling, Immunohistochemistry, and Immunofluorescence Microscopy—Hearts were arrested in diastole and perfusion-fixed with 4% paraformaldehyde and embedded in paraffin, sectioned at 6 μm, and stained with hematoxylin and eosin, Sirius red, or fluorescein isothiocyanate-labeled wheat germ agglutinin (WGA). Slides were visualized using a Nikon Eclipse E600 microscope and a Zeiss Axiovert 135 for immunofluorescence. Cell surface areas were determined using SPOT-imaging software (Diagnostic Instruments). Sections were immunolabeled with the following: Mac3 (1:30, Pharmingen) to detect macrophages; CD31 monoclonal antibody (1:50, Pharmingen) to detect capillaries, and CD45 (1:30, Pharmingen) to detect leukocytes.

Quantitative RT-PCR—Total RNA was isolated using TRIzol reagent (Invitrogen). One μg of RNA was used as template for Superscript reverse transcriptase II (Promega) using indicated primer combinations (primer sequences available upon request). For real time RT-PCR, the Bio-Rad iCycler (Bio-Rad) and SYBR Green was used as described in detail previously (20) and as described in detail in the supplemental Expanded Methods.

Cage-wheel Exercise—Male *nfatc2*$^{-/-}$ *and nfatc2*$^{+/+}$ mice were subjected to voluntary cage wheel exercise (21) Briefly, individual animals were individually housed in a cage equipped with an 11.5-cm-diameter running wheel with a 5.0-cm-wide running surface equipped with a digital magnetic counter activated by wheel rotation. Daily exercise values for time and distance run were recorded for individual exercised animals throughout the duration of the exercise period (4 weeks).

Statistical Analysis—The results are presented as means ± S.E. Statistical analyses were performed using INSTAT 3.0 software (GraphPad) and consisted of analysis of variance, followed by Tukey's post-test when group differences were detected at the 5% significance level or the Student *t* test when two experimental groups were compared. Statistical significance was accepted at a p value <0.05.

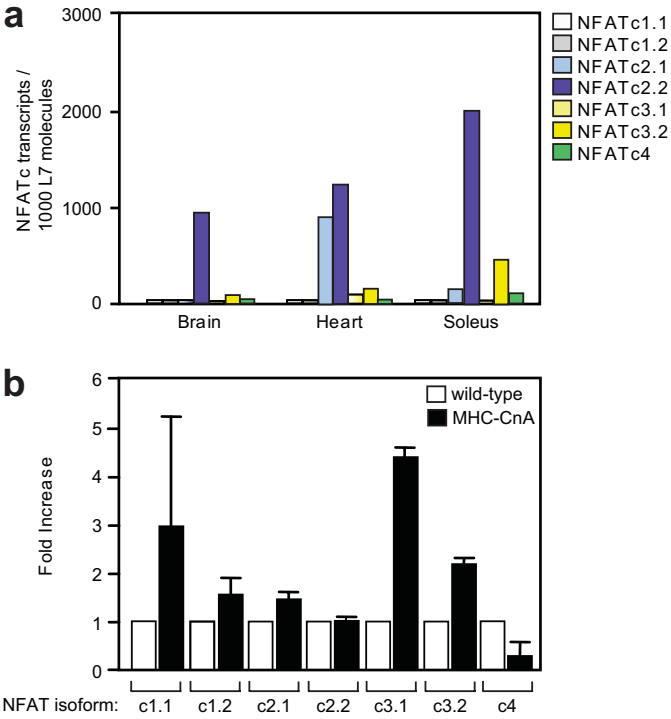

FIGURE 1. **NFAT splice isoform distribution in excitable tissues.** *a*, quantitative assessment of transcript abundance of different NFAT (splice) isoforms in murine brain, heart, and soleus muscle, normalized to the relative abundance of transcripts for 60 S ribosomal protein L7 (depicted is the average of $n = 3$ per group). *b*, detection of NFAT autoregulation in hearts with calcineurin activation. The data demonstrate that upon calcineurin/NFAT activation, *nfatc1.1*, *nfatc3.1*, and *nfatc3.2* splice transcripts are relatively enriched compared with base line, and *nfatc4* transcripts decrease ($n = 3$ per group).

RESULTS

NFATc2 Is the Most Abundant Isoform in the Mouse Heart—Recently, we demonstrated that all four calcineurin-regulated members of the NFAT family (NFATc1–c4) exist in cardiomyocytes (14, 15). Members of the NFAT transcription factor family are expressed as in multiple spliced transcripts (22–24). We analyzed the relative abundance of NFAT (splice) transcripts using quantitative RT-PCR, because commercially available antibodies against NFAT (splice) isoforms are qualitatively weak and unsuitable to provide relative NFAT isoform protein quantities. We found that transcripts for *nfatc2* are the most abundant in excitable tissues such as brain, soleus muscle, and heart (Fig. 1*a*).

nfat genes can have redundant, overlapping functions in distinct organs. To analyze whether auto-amplification of *nfat* isoforms may exist in the heart, we quantified their transcripts in hearts from wild-type mice and transgenic mice harboring a constitutively active mutant of calcineurin under control of the *Myh6* promoter (MHC-CnA), leading to a profound hypertrophy response in juvenile mice and fulminant heart failure at adulthood (5, 25). The results indicate that *nfat* transcript distribution remains relatively similar, except for slight increases

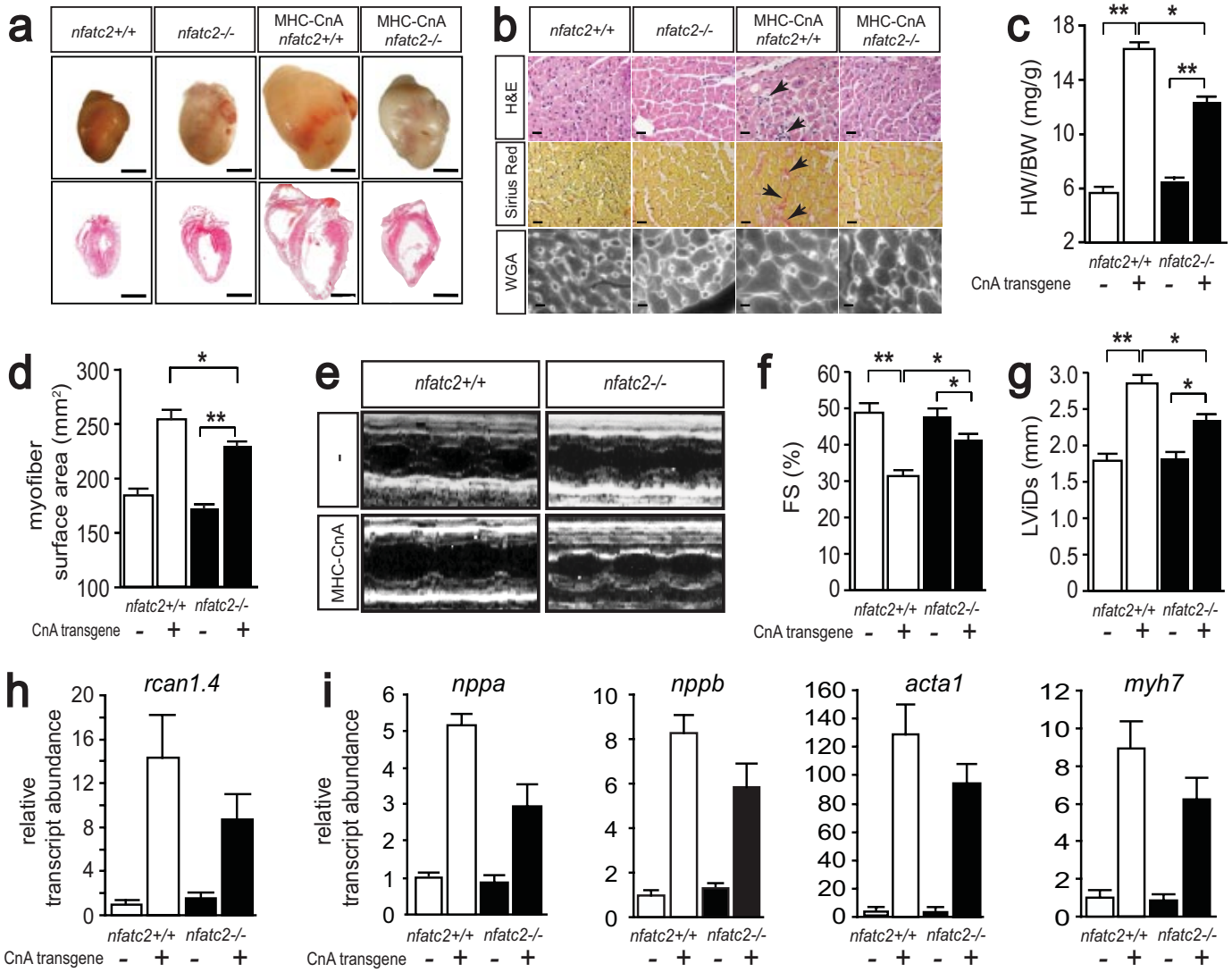

FIGURE 2. **Gravimetrical, histological, functional, and molecular analysis of calcineurin-transgenic mice crossed into a *nfatc2*-null background.** *a,* representative gross morphology and hematoxylin and eosin-stained four-chamber view of hearts dissected from 3-week-old mice of indicated genotypes, demonstrating a profound rescue of cardiac enlargement by *nfatc2* ablation downstream of calcineurin activation (*bar,* 5 mm). *b,* representative histological images of hearts from mice with genotypes indicated under *a* (*bar,* 0.2 mm). Hematoxylin and eosin (*H&E*)-stained images reveal remarkable myocyte hypertrophy, myofiber disarray, and cellular infiltrates (*arrowheads*) in MHC-CnA/*nfatc2*$^{+/+}$ mice, whereas MHC-CnA/*nfatc2*$^{-/-}$ mice are largely protected against these structural alterations. Sirius red staining indicates massive interstitial and perivascular fibrosis in hearts of MHC-CnA/*nfatc2*$^{+/+}$ mice, which is attenuated in MHC-CnA/*nfatc2*$^{-/-}$ mice. Wheat germ agglutinin staining reveals a significant increase in cardiomyocyte size in MHC-CnA/*nfatc2*$^{+/+}$ mice compared with *nfatc2*$^{+/+}$ and *nfatc2*$^{-/-}$ mice, and myofiber size of the MHC-CnA/*nfatc2*$^{-/-}$ mice was visibly smaller. *c,* heart weight/body weight ratios of 3-week-old *nfatc2*$^{+/+}$, *nfatc2*$^{-/-}$, MHC-CnA/*nfatc2*$^{+/+}$, and MHC-CnA/*nfatc2*$^{-/-}$ mice ($n = 5$ per group). *d,* quantification of myofiber cross-sectional area from indicated genotypes shows significant attenuation of myocyte hypertrophy in MHC-CnA/*nfatc2*$^{-/-}$ mice compared with MHC-CnA/*nfatc2*$^{+/+}$ mice ($n = 3$ per group, with 100 fibers counted per animal). *e,* representative M-mode images of *nfatc2*$^{+/+}$, *nfatc2*$^{-/-}$, MHC-CnA/*nfatc2*$^{+/+}$, and MHC-CnA/*nfatc2*$^{-/-}$ mice at 4 weeks of age, indicating dilation and loss of contractile behavior in MHC-CnA/*nfatc2*$^{+/+}$ mice, which was substantially attenuated in MHC-CnA/*nfatc2* null mice ($n = 4–6$ per group). *f* and *g, bar graph* representations of fractional shortening (*FS*) and LVID at systole, indicating protection against functional and geometrical deterioration after TAC compared with *nfatc2*$^{+/+}$ mice ($n = 4–6$ per group). *h* and *i,* real time PCR analysis for *rcan1.4* (*h*) and hypertrophic markers (*i*), all of which were increased in MHC-CnA/*nfatc2*$^{+/+}$ mice and repressed in MHC-CnA/*nfatc2*$^{-/-}$ mice ($n = 3–5$ per group). *, $p < 0.05$; **, $p < 0.01$.

in NFATc1.1, NFATc3.1, and NFATc3.2 and a relative decrease in NFATc4 compared with unstimulated hearts (Fig. 1*b*). Collectively, these data indicate that *nfatc2* transcripts outnumber those from other *nfat* genes in the unstimulated heart by severalfold and that mild auto-amplification loops involving *nfatc1* and *nfatc3* exist following calcineurin signaling.

NFATc2 Is Required for Calcineurin-induced Cardiac Hypertrophy—The transcriptional mechanisms whereby calcineurin initiates or maintains pathological hypertrophy *in vivo* are still ill defined. To determine the relevance of the relative abundance of *nfatc2* transcripts downstream of calcineurin signaling in the postnatal heart, we crossbred *nfatc2*-null mice with MHC-CnA mice. At 3 weeks of age, *nfatc2*$^{+/+}$ and *nfatc2*$^{-/-}$ mice displayed comparable gross morphology and equal HW/BW ratios, a standardized measure of cardiac hypertrophy (5.6 ± 0.4 and 6.2 ± 0.4 mg/g, respectively). In contrast, MHC-CnA/*nfatc2*$^{+/+}$ mice displayed grossly enlarged atrial and ventricular chambers, biventricular dilation, and a tripling of the HW/BW ratio (16.9 ± 0.6 mg/g; Fig. 2, *a* and *c*). Remarkably, MHC-CnA mice harboring a null mutation for the *nfatc2*

gene displayed a visible reduction in cardiac enlargement (11.5 ± 0.6 mg/g; Fig. 2*b*), which constitutes a decrease of 53% in HW/BW ratios compared with MHC-CnA/*nfatc2*$^{+/+}$ mice. Body weights were not different between the four experimental cohorts (12.4 ± 1.0, 12.6 ± 0.9, 13.2 ± 0.9, and 12.0 ± 0.3 g, not significant for *nfatc2*$^{+/+}$, *nfatc2*$^{-/-}$, MHC-CnA/*nfatc2*$^{+/+}$, and MHC-CnA/*nfatc2*$^{-/-}$ mice, respectively).

Histopathological analysis from hematoxylin and eosin-, Sirius red-, and wheat germ agglutinin (WGA)-stained cardiac sections revealed cardiomyocyte hypertrophy, myocyte disarray, mild invasion of inflammatory infiltrates, and extensive areas of interstitial and perivascular fibrosis were evident in MHC-CnA/*nfatc2*$^{+/+}$ hearts, whereas MHC-CnA/*nfatc2*$^{-/-}$ mice did not display these abnormalities (Fig. 2*b*). As a more quantitative evaluation of individual myofiber hypertrophy, myofibril cross-sectional areas were quantified from WGA-stained sections. *nfatc2*$^{+/+}$ and *nfatc2*-null mice had similar myofiber cross-sectional areas, whereas MHC-CnA/*nfatc2*$^{+/+}$ mice had significantly increased individual myofibril size (Fig. 2*d*). In contrast, a 47% reduction was observed in MHC-CnA mice lacking *nfatc2*. These data confirm that loss of *nfatc2* attenuates calcineurin-induced cardiac hypertrophy.

To examine the impact of *nfatc2* ablation on calcineurin-induced hemodynamic dysfunction, all cohorts were subjected to serial two-dimensional and M-mode echocardiography at 4 weeks of age. Representative images of M-mode recordings are displayed in Fig. 2*e*. An increase in left ventricular internal diameter (LVID) and a proportional decrease in systolic contractility (FS) were evident in the MHC-CnA/*nfatc2*$^{+/+}$ mice, whereas these parameters were clearly improved in MHC-CnA/*nfatc2*$^{-/-}$ animals (Fig. 2, *f* and *g*).

Transcript abundance of the exon 4 splice isoform of *rcan1* (regulator of calcineurin-1) may reflect a quantitative measure of total NFAT activity downstream of calcineurin signaling in the heart (12). Transcripts for *rcan1.4* were substantially up-regulated in MHC-CnA/*nfatc2*$^{+/+}$ mice and reduced to 50% in MHC-CnA/*nfatc2*$^{-/-}$ hearts (Fig. 2*h*). Likewise, reactivation of fetal gene expression is a hallmark of pathological hypertrophy and heart failure, and therefore the expression levels of a number of fetal genes were determined. Transcripts for *nppa* (atrial natriuretic factor), *nppb* (brain natriuretic peptide), and *myh7* (β-myosin heavy chain) were substantially repressed upon *nfatc2* deletion (Fig. 2*i*). In conclusion, these results indicate that loss of *nfatc2* led to a significant reduction of all major calcineurin-induced structural alterations in the myocardium.

Nfatc2-deficient mice display modest splenomegaly, hyperproliferation of T- and B-cells, and dysregulated interleukin-4 production (17, 26). To exclude the possibility that the observed cardiac phenotype was indirectly related to the relative immunodeficiency because of loss of NFATc2, we analyzed histological sections of hearts from the experimental groups for macrophages (MAC3) and leukocytes (CD45). Cardiac sections of *nfatc2*-null mice showed no increase in numbers of macrophages and infiltrated leukocytes (supplemental Figure). Likewise, NFATc2 was shown to promote angiogenesis by regulating c-Flip expression (27). To ascertain that *nfatc2* ablation did not influence the cardiac phenotype by dysregulating the myocardial angiogenic potential, we analyzed capillary densities in cardiac sections by staining with CD31 (supplemental Figure). We did not observe a difference in capillary density in cardiac sections of *nfatc2*-null mice, MHC-CnA transgenic mice, or wild-type mice. These results indicate that *nfatc2* deficiency produces a fundamental deficit in the ability of calcineurin to execute a full myocyte hypertrophy response.

NFATc2 Deficiency Compromises Pathophysiologic Cardiac Hypertrophy—To determine whether NFATc2 also regulates hypertrophy in response to more physiologic stimuli apart from transgenic stimuli, continuous angiotensin II infusion was performed. Vehicle-treated *nfatc2*$^{+/+}$ and *nfatc2*$^{-/-}$ mice displayed similar HW/BW ratios (4.1 ± 0.1 and 4.3 ± 0.1 mg/g, respectively). In response to angiotensin II, *nfatc2*-null mice still developed some degree of hypertrophy, although this was significantly blunted compared with the response displayed by *nfatc2*$^{+/+}$ mice (Fig. 3, *a* and *b*).

Next, TAC banding was performed, a surgical technique where the aorta was partially constricted for 1 week to mimic chronic hypertensive disease in humans. To validate that the surgical procedure produced equal pressure gradients in all experimental groups, transcarotid pressures were measured invasively (Fig. 3*c*). Sham-operated *nfatc2*$^{+/+}$ and *nfatc2*$^{-/-}$ mice displayed similar HW/BW ratios (4.7 ± 0.1 and 5.3 ± 0.1 mg/g, respectively). In response to TAC, *nfatc2*-null mice still developed some degree of hypertrophy, although this was significantly blunted compared with the response displayed by *nfatc2*$^{+/+}$ mice. This was further reflected in HW/BW ratios (6.0 ± 0.1 and 6.9 ± 0.2 mg/g, respectively; Fig. 3*d*), indicating that ablation of one single *nfat* isoform was sufficient to abrogate the early cardiac growth response by 68% in response to hemodynamic loading. Body weights were not different between the groups (28.3 ± 0.3, 25.4 ± 2.3, 27.8 ± 0.6, and 26.3 ± 1.2 g, not significant, for *nfatc2*$^{+/+}$ and *nfatc2*$^{-/-}$ sham and *nfatc2*$^{+/+}$ and *nfatc2*$^{-/-}$ TAC, respectively).

Hematoxylin and eosin- and Sirius red-stained cardiac histological sections did not show any signs of histopathology in *nfatc2*$^{+/+}$ and *nfatc2*$^{-/-}$ sham-operated mice. In contrast, cardiomyocyte hypertrophy, myocyte disarray, mild invasion of inflammatory infiltrates, and extensive areas of interstitial and perivascular fibrosis were evident in pressure-overloaded *nfatc2*$^{+/+}$ hearts, whereas *nfatc2*$^{-/-}$ mice displayed these abnormalities in a much milder form in response to TAC (Fig. 3, *e* and *f*). Myofibril cross-sectional areas were quantified from WGA-stained histological sections. *nfatc2*$^{+/+}$ and *nfatc2*$^{-/-}$ sham-operated mice had similar myofiber cross-sectional areas (232 ± 7 and 256 ± 4 mm^2, respectively), whereas pressure-overloaded *nfatc2*$^{-/-}$ mice had significantly decreased individual myofibril size compared with *nfatc2*$^{+/+}$ mice after TAC surgery (434 ± 10 and 588 ± 14 mm^2, respectively). These data confirm that loss of *nfatc2* reduced pressure overload-induced myofibril hypertrophy (Fig. 3*f*).

Reactivation of fetal gene expression is a hallmark of pathological hypertrophy and heart failure, and therefore the expression levels of a number of fetal genes were determined. Transcripts for *nppa* (atrial natriuretic factor), *nppb* (brain natriuretic peptide), and *myh7* (β-myosin heavy chain) were substantially repressed upon pressure overload in *nfatc2*-null mice compared with wild-type controls (Fig. 3*g*). Collectively,

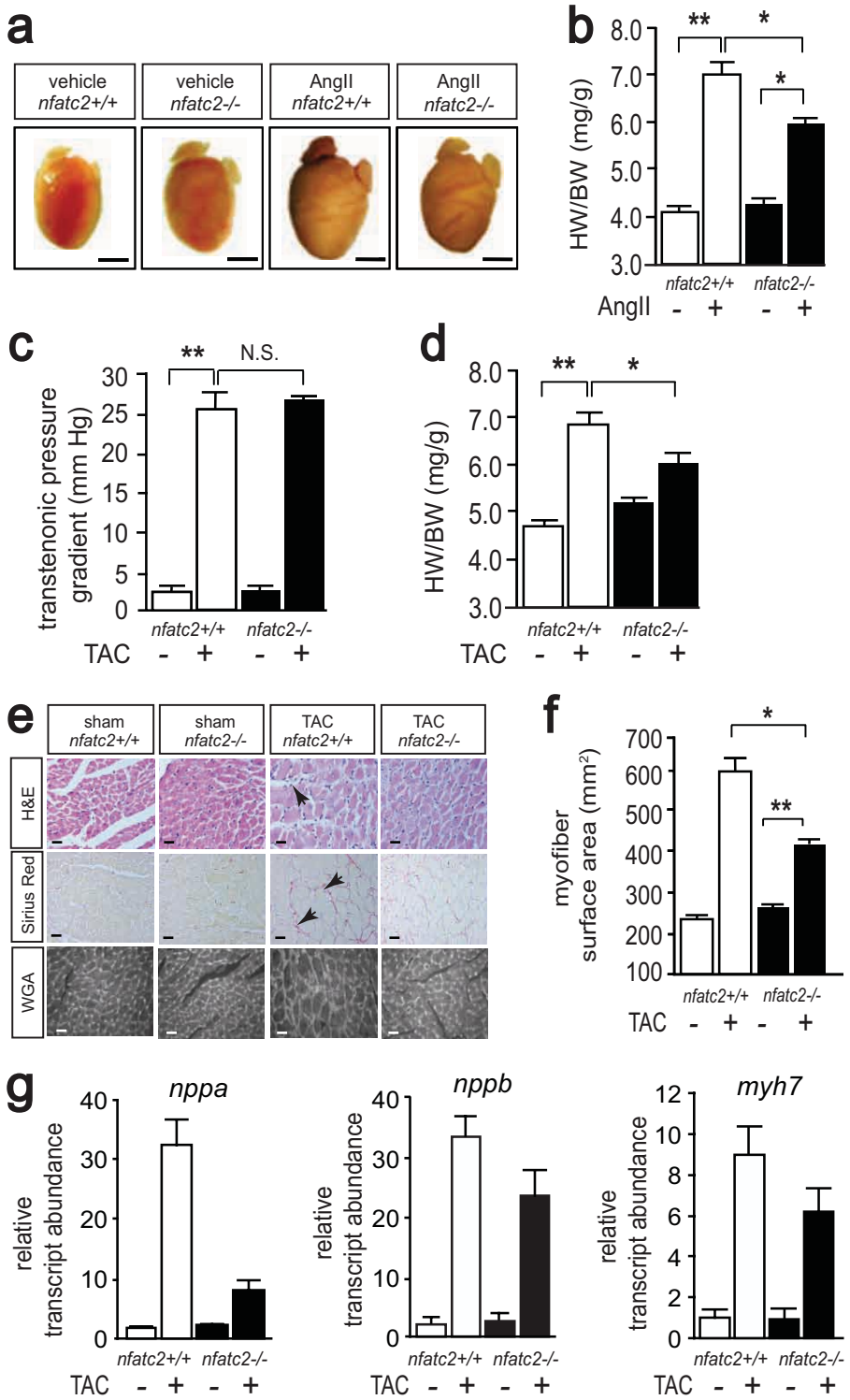

FIGURE 3. **Nfatc2 ablation attenuates agonist-induced and pressure overload-induced cardiac hypertrophy.** *a,* representative gross morphology of hearts dissected from mice of indicated genotypes continuously infused with angiotensin II (*AngII*) or vehicle, demonstrating a profound rescue of cardiac enlargement by *nfatc2* ablation (*bar,* 5 mm). *b,* heart weight to body weight (*HW/BW*) ratios of indicated genotypes show a decreased hypertrophic response for *nfatc2*$^{-/-}$ hearts compared with wild-type hearts after 2 weeks of vehicle or angiotensin II infusion ($n = 6$ per group). *c,* pressure gradients across the proximal and distal transverse aorta were measured invasively to validate the TAC procedure. *d,* HW/BW ratios of indicated genotypes subjected to sham or TAC surgery show a decreased hypertrophic response for *nfatc2*$^{-/-}$ hearts compared with wild-type hearts after 1 week of TAC ($n = 6$ per group). *e,* hematoxylin and eosin (*H&E*), Sirius red, and WGA staining indicates an increase in myocyte hypertrophy, myofiber disarray, cellular infiltrates (*arrowheads*), accumulation of interstitial and perivascular fibrosis, and increased myofibercross-sectional areas in *nfatc2*$^{+/+}$ mice subjected to TAC compared with sham-operated genotypes, whereas this was attenuated in *nfatc2*$^{-/-}$ mice subjected to TAC. *f,* quantification of myofiber cross-sectional areas from WGA-stained sections of indicated genotypes ($n = 3$ per genotype, with 100 fibers counted per animal). *g,* real time PCR analysis for hypertrophic markers, all of which were increased in *nfatc2*$^{+/+}$ TAC mice and repressed in *nfatc2*$^{-/-}$ mice subjected to TAC ($n = 3$ per group). *N.S.*, not significant; *, $p < 0.05$; **, $p < 0.01$.

these results demonstrate a clear defect in the structural and molecular program of pathological cardiac hypertrophy in the absence of *nfatc2*.

NFATc2 Deficiency Ameliorates Heart Failure—To test whether sustained attenuation of pressure-overload hypertrophy ameliorates cardiac function and ensuing heart failure development in the absence of *nfatc2*, we performed TAC on *nfatc2*$^{+/+}$ and *nfatc2*$^{-/-}$ mice for 8 weeks. To ensure equal loading conditions on all experimental groups, pressure gradients were measured noninvasively (Fig. 4*a*). At 8 weeks, gross morphology showed no differences between sham-operated *nfatc2*$^{+/+}$ and *nfatc2*$^{-/-}$ mice (HW/BW ratios of 4.1 ± 0.2 and 4.4 ± 0.2 mg/g, respectively, not significant; see Fig. 4, *b* and *c*). In contrast, substantial cardiac enlargement was evident in *nfatc2*$^{+/+}$ mice at 8 weeks after TAC surgery, whereas *nfatc2*$^{-/-}$ mice had visibly smaller hearts (Fig. 4, *b* and *c*). This was further reflected by HW/BW ratios (6.2 ± 0.3 and 5.8 ± 0.2 mg/g, respectively, $p < 0.05$; see Fig. 4*c*), indicating that *nfatc2*$^{-/-}$ mice displayed a sustained reduction in cardiac hypertrophy over longer periods of pressure overload. Hematoxylin and eosin staining showed no myocyte disarray or infiltration of inflammatory cells in both sham groups. Pressure overloaded *nfatc2*$^{-/-}$ hearts showed less myocyte disarray and infiltration in sections compared with pressure-overloaded *nfatc2*$^{+/+}$ hearts (Fig. 4*g*). Sirius red staining of hearts demonstrated a profound reduction in fibrosis in pressure-overloaded *nfatc2*$^{-/-}$ hearts compared with pressure overloaded *nfatc2*$^{+/+}$ hearts (Fig. 4*g*).

To examine the impact of *nfatc2* ablation on pressure overload-induced hemodynamic behavior, all cohorts were subjected to serial two-dimensional and M-mode echocardiography at 2, 4, 6, and 8 weeks after TAC. Representative images of M-mode recordings at 4 and 8 weeks are displayed in Fig. 4*d*. Four weeks after TAC, an increase in LVID (Fig. 4, *d* and *e*) and a proportional decrease in systolic contractility (FS) were evident in the *nfatc2*$^{+/+}$ mice subjected to pressure overload (Fig. 4, *d* and *f*), in contrast to *nfatc2*-null animals. At 8 weeks after TAC, a thickening of the posterior wall in diastole, further increases in LVID, and progressive decreases in FS were visible in *nfatc2*$^{+/+}$ mice, indicative of progressive left ventricular dilation and heart failure (Fig. 4*e* and Table 1). *nfatc2*-deficient mice displayed a significant reduction of these geometrical and functional deteriorations (Fig. 4, *d–f*, and Table 1). Taken together, these results indicate that *nfatc2* deficiency not only protects the heart from pathological hypertrophy but also efficiently counteracts myocardial functional deterioration following biomechanical stress.

NFATc2 Ablation Does Not Affect Physiological Cardiac Hypertrophy—One vexing question relates to whether genetically distinct molecular mechanisms are employed to achieve pathological *versus* athletic cardiac enlargement, because the latter form of cardiac growth does not provoke hemodynamic demise or predisposes to heart failure. To this end, we chose voluntary running-wheel exercise (21) as a model to stimulate physiological cardiac hypertrophy in cohorts of *nfatc2*$^{+/+}$ and *nfatc2*$^{-/-}$ mice. After 4 weeks of voluntary wheel exercise, *nfatc2*$^{-/-}$ mice were able to generate a cardiac growth response identical to that observed in *nfatc2*$^{+/+}$ mice as evidenced by their HW/BW ratios (Fig. 5, *b* and *c*). As expected, exercised *nfatc2*$^{+/+}$ *or nfatc2*$^{-/-}$ mice did not display any evidence of histopathology despite a 40% increase in heart weight. Our results indicate that calcineurin-NFAT signaling is not activated after voluntary wheel running, given that the hypertrophy response was not rescued in *nfatc2* null mice.

DISCUSSION

Functional Hierarchy among Cardiac NFAT Isoforms in Cardiac Pathology—One unanticipated finding of this study is the relative high abundance of the NFATc2 isoform in cardiac muscle. Calcineurin-regulated members of the NFAT family (NFATc1–c4) are encoded by four separate genes and expressed as multiple spliced transcripts in rodents and human (13, 22–24). Recently, we demonstrated the existence of proteins for all four NFATc isoforms in cardiomyocytes (14, 15). Here, we analyzed the relative abundance of NFAT (splice) transcripts, because most commercially available antibodies proved ineffective to quantify the relative abundance of the low levels of NFAT proteins in the adult heart (15).

Here we show that mRNAs for *nfatc4* and *nfatc1* are relatively less abundant in the heart. Indeed, *nfatc4*-null mice harboring a cardiac specific calcineurin transgene did not display a compromise of cardiac hypertrophy and heart failure (15). In contrast, transcripts for *nfatc3* and *nfatc2* are relatively most abundant in the heart, with the latter still present at several -fold more than those for *nfatc3*. *nfatc3*-null mice are also partially deficient in their ability to undergo cardiac hypertrophy (15). In this study, we show that *nfatc2*-null mice display abrogation of calcineurin-provoked cardiac growth and a clear protection against the geometrical, functional, and molecular deterioration of the myocardium following hemodynamic loading. The combined findings imply predominant roles for *nfatc2* and *nfatc3*, in the execution of cardiac remodeling and heart failure downstream of calcineurin. The collective findings would also suggest that mice deficient for both *nfatc2* and *nfatc3* might display an even more complete inhibition of calcineurin-mediated cardiac hypertrophy and heart failure. Conversely, given previous findings with *nfatc4*-null mice (15) and the very low transcripts levels for *nfatc1* and *nfatc4* we detected in this study, the combined observations also suggest that latter *nfat* isoforms have very little impact on calcineurin-dependent hypertrophy (15).

NFAT proteins can have redundant, overlapping functions in distinct organs. Indeed, NFATc1 and NFATc2 are involved in an autoregulatory mechanism controlling bone homeostasis by inducing transcription of *nfatc1* by NFAT through its promoter region (28). We found that in the heart NFAT transcript distribution remains relatively similar, except for slight increases in NFATc1.1, NFATc3.1, and NFATc3.2 mRNA, and a relative decrease in NFATc4 mRNA compared with unstimulated hearts. The functional ramifications of this transcript redistribution remain unknown. Collectively, the data indicate that *nfatc2* transcripts outnumber those from other *nfat* genes in the heart by severalfold and that mild auto-amplification loops involving *nfatc1* and *nfatc3* exist following calcineurin activation.

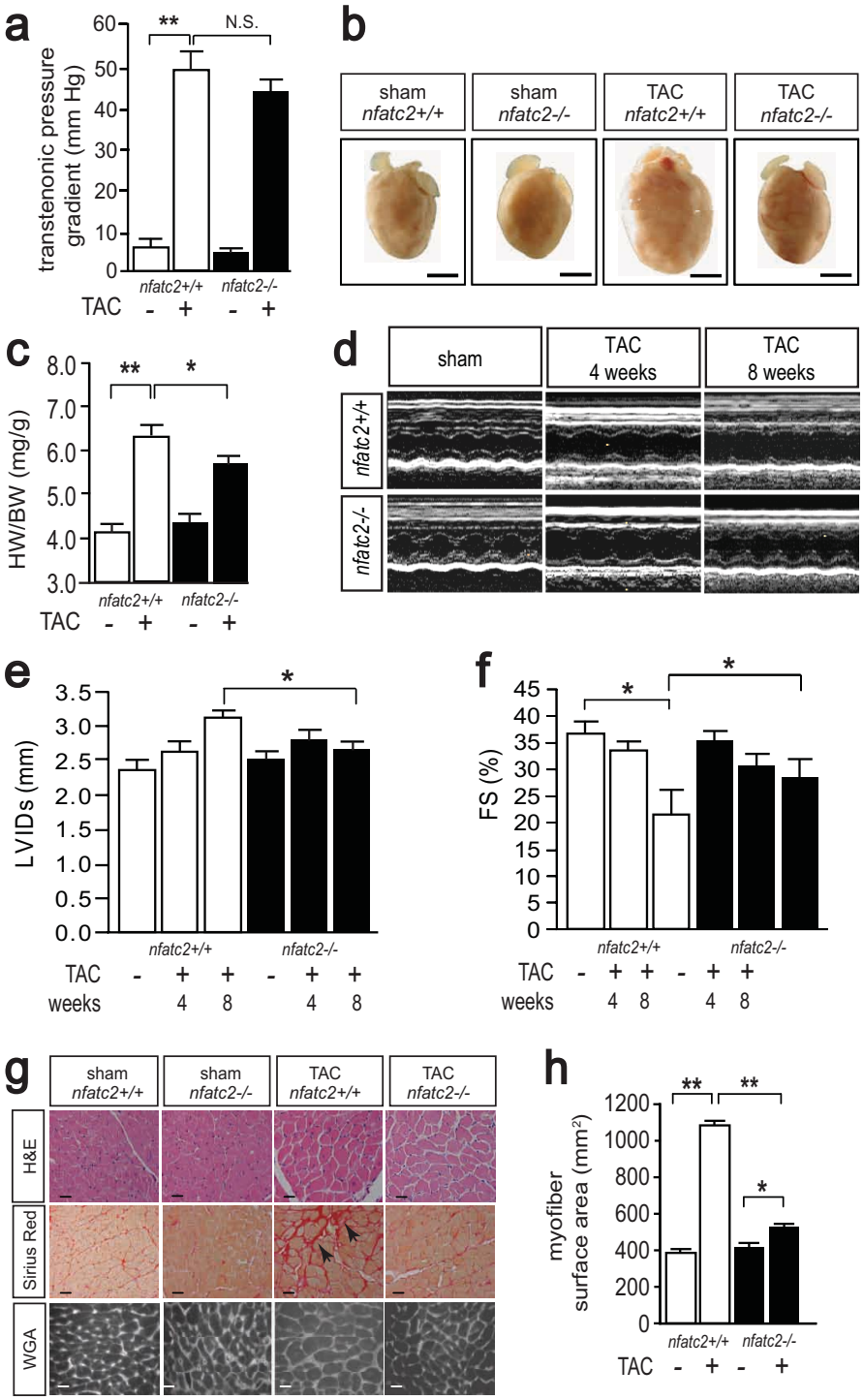

FIGURE 4. **Nfatc2 deficiency prevents pressure overload-induced heart failure.** *a,* pressure gradients across the proximal and distal transverse aorta were measured noninvasively to validate the TAC procedure. *b,* representative gross morphology of hearts dissected from mice of indicated genotypes subjected to 8 weeks of TAC, indicating profound rescue of cardiac enlargement by *nfatc2* deletion (*bar,* 5 mm). *c,* heart weight to body weight (*HW/BW*) ratios of indicated genotypes subjected to sham or TAC surgery show a decreased hypertrophy response for $nfatc2^{-/-}$ hearts compared with wild-type hearts after 8 weeks of TAC ($n = 6–10$ per group). *d,* representative M-mode images of sham or TAC $nfatc2^{+/+}$ and $nfatc2^{-/-}$ mice at 4 and 8 weeks indicates progressive dilation and loss of contractile behavior in $nfatc2^{+/+}$ mice, which was substantially attenuated in *nfatc2* null mice. *e* and *f, bar graph* representations of fractional shortening (*FS*) and left ventricular internal diameter at systole (*LVIDs*), indicating protection against functional and geometrical deterioration after TAC compared with $nfatc2^{+/+}$ mice ($n = 6–10$ per group). *g,* hematoxylin and eosin (*H&E*), Sirius red, and WGA staining indicates an increase in myocyte hypertrophy, myofiber disarray, cellular infiltrates (arrowheads), accumulation of interstitial and perivascular fibrosis, and increased myofibercross-sectional areas in $nfatc2^{+/+}$ mice subjected to 8 weeks of TAC compared with sham-operated genotypes, whereas this was attenuated in $nfatc2^{-/-}$ mice subjected to TAC. *h,* quantification of myofiber cross-sectional areas from WGA-stained sections of indicated genotypes ($n = 3$ per genotype, with 100 fibers counted per animal). *N.S.*, not significant; *, $p < 0.05$; **, $p < 0.01$.

NFAT Signaling Is Genetically Restricted to Pathological Cardiac Growth and Maladaptive in Nature—Classical conceptualization has it that left ventricular hypertrophy would start as an adaptive, beneficial response to normalize wall stress to either altered mechanical loading conditions (*e.g.* resulting from valvular disease or chronic hypertension) or decreased performance because of loss of contractile units (*e.g.* after ischemic heart loss), and only later acquires maladaptive characteristics. Following this interpretation, increased wall thickness serves as the means to restore wall stress in line with the law of Laplace (29).

Recent insights have demanded a more nuanced interpretation of this phenomenon of "compensatory hypertrophy" and the absolute need to restore wall stress to prevent hemodynamic demise (12, 30, 31). First, ventricular hypertrophy is demonstrably a risk factor for cardiovascular mortality in humans (32). Second, beyond just increased mass, the specific long term transcriptional responses to increased load entail a myriad of quantitative and qualitative changes in cardiac gene expression that are reminiscent of fetal cardiac myocytes. In patients with cardiac failure, functional improvement related to treatment with β-blockers is correlated with beneficial changes in myocardial gene expression, most prominently exemplified by a correction in the mRNA expression level of the β-MHC gene (33). In this study we noted a pronounced decrease in β-MHC gene expression in *nfatc2*-null mice compared with their wild-type counterparts after hemodynamic loading. Conclusively, Laplace's Law, although conceptually sound, does not take into account the qualitative alterations of the wall, and only incompletely explains the phenotypic particulars of heart enlargement.

In most models of pathological hypertrophy studied to date, inhibition of the calcineurin/NFAT axis has yielded either a reduction in the hypertrophic response and/or a delay in the progression from hypertrophy to heart failure (5–12). The data presented in this study extend this paradigm and demonstrate that NFAT transcriptional activity is activated in a sustained manner during pressure overload-induced cardiac remodeling and heart failure. Our results also provide genetic evidence that NFATc2 is not required for hypertrophic growth of the heart in response to exercise because heart weight remained unaffected in *nfatc2*-null mice following voluntary wheel running. These data are in line with earlier findings in a transgenic mouse model harboring an NFAT-sensitive luciferase reporter, which was selectively regulated by pathological hypertrophic remodeling and not by forced swimming exercise as a model to provoke physiological hypertrophy (34).

Because cardiac sections of wild-type and *nfatc2* null mice did not show differences in infiltrating macrophages or leukocytes, nor displayed differences in capillary

TABLE 1

Echocardiographic and morphometric characteristics in wild-type and *nfatc2*-null mice 8 weeks after TAC

Data are expressed as mean ± S.E. Awths is anterior wall thickness in systole; Awthd is anterior wall thickness in diastole; PWths is posterior wall thickness in systole; PWthd is posterior wall thickness in diastole; LVIDs is left ventricular internal diameter in systole; LVIDd is left ventricular internal diameter in diastole; PWths is posterior wall thickness in systole; PWthd is posterior wall thickness in diastole; FS is fractional shortening; Lvmass is echocardiography-derived left ventricular mass; HW is post-mortem heart weight; BW is post-mortem body weight; TL is post-mortem tibial length; HW/BW is heart weight to body weight ratio; HW/TL is heart weight to tibial length ratio.

	Sham		TAC	
	nfatc2$^{+/+}$, *n* = 6	*nfatc2*$^{-/-}$, *n* = 6	*nfatc2*$^{+/+}$, *n* = 8	*nfatc2*$^{-/-}$, *n* = 7
Echo				
DeltaP, mm Hg	7 ± 2	6 ± 1	50 ± 4[a]	44 ± 3[a]
AWths, mm	1.6 ± 0.1	1.4 ± 0.1	1.6 ± 0.1	1.5 ± 0.1
AWthd, mm	1.2 ± 0.1	1.1 ± 0.1	1.2 ± 0.1	1.1 ± 0.1
LVIDs, mm	2.6 ± 0.1	2.5 ± 0.1	3.0 ± 0.1[a]	2.7 ± 0.1[a,b]
LVIDd, mm	3.6 ± 0.1	3.7 ± 0.1	4.0 ± 0.1[a]	3.7 ± 0.2[b]
PWths, mm	1.1 ± 0.1	1.1 ± 0.1	1.2 ± 0.1	1.3 ± 0.1
PWthd, mm	1.0 ± 0.1	1.0 ± 0.1	1.0 ± 0.1	1.1 ± 0.1
FS (%)	37 ± 2	35 ± 2	22 ± 5[a]	28 ± 4[a,b]
LVmass (mg)	116 ± 7	117 ± 11	153 ± 11[a]	130 ± 14[a,b]
Morphometry				
HW (mg)	127 ± 4	136 ± 8	193 ± 11[a]	171 ± 7[a,b]
BW (g)	32 ± 1	31 ± 1	31 ± 1	30 ± 1
TL (mm)	19 ± 1	18 ± 1	18 ± 1	18 ± 1
HW/BW (mg/g)	4.1 ± 0.2	4.4 ± 0.2	6.2 ± 0.3[a]	5.8 ± 0.2[a,b]
HW/TL (mg/mm)	6.8 ± 0.2	7.6 ± 0.5	10.8 ± 0.7[a]	9.5 ± 0.4[a,b]

[a] Values indicate $p < 0.05$ *versus* corresponding sham-operated group.
[b] Values indicate $p < 0.05$ *versus* wild-type group after TAC.

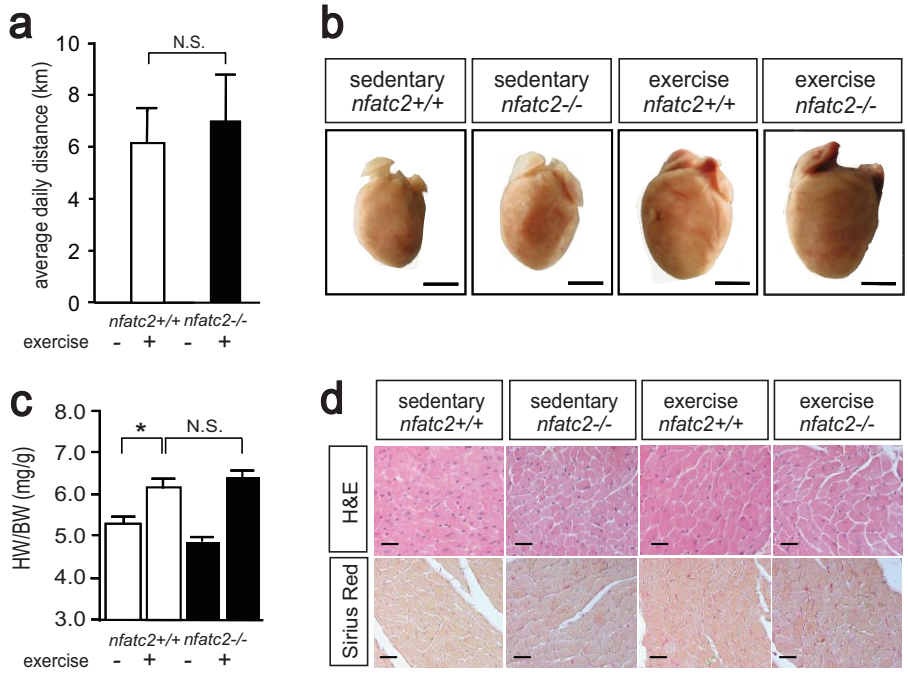

FIGURE 5. **Nfatc2 deficiency does not affect physiological hypertrophy.** *a,* average daily distance that mice ran voluntarily. *b,* representative gross morphology from sedentary and exercised mice, indicating that exercised *nfatc2*$^{+/+}$ and *nfatc2*$^{-/-}$ develop equal cardiac enlargement. *c,* heart weight to body weight (*HW/BW*) ratios of indicated genotypes either sedentary or exercised ($n = 8$ per group). *d,* representative hematoxylin and eosin (*H&E*) and Sirius staining of heart sections of indicated genotypes indicates no histopathological alterations following exercise. *N.S.*, not significant; *, $p < 0.05$.

density, we conclude that *nfatc2* deficiency produces a fundamental deficit in the cardiac myocyte to execute a full hypertrophy response. Nevertheless, we cannot fully exclude the possibility that nonmyocyte-related effects secondary to systemic loss of *nfatc2* may have influenced the cardiac phenotypes we observed. Combined, these data demonstrate that NFAT transcriptional activity is a required genetic pathway and selectively activated in pathological hypertrophy and ensuing heart failure. Furthermore, this study suggests that approaches targeting either NFATc2 activation or its immediate downstream target genes provide a suitable approach for future drug design to treat forms of pathological cardiac hypertrophy and heart failure.

Acknowledgments—We are grateful to Eric Olson and Laurie Glimcher for sharing mouse models and Jeroen Korving, Jennifer Megan Meerding, and Pantelis Hatizis for technical assistance.

REFERENCES

1. Ho, K. K., Pinsky, J. L., Kannel, W. B., and Levy, D. (1993) *J. Am. Coll. Cardiol.* **22,** Suppl. 4, 6A–13A
2. Lloyd-Jones, D. M., Larson, M. G., Leip, E. P., Beiser, A., D'Agostino, R. B., Kannel, W. B., Murabito, J. M., Vasan, R. S., Benjamin, E. J., and Levy, D. (2002) *Circulation* **106,** 3068–3072
3. Oakley, D. (2001) *Heart* **86,** 722–726
4. Olson, E. N., and Schneider, M. D. (2003) *Genes Dev.* **17,** 1937–1956
5. Molkentin, J. D., Lu, J. R., Antos, C. L., Markham, B., Richardson, J., Robbins, J., Grant, S. R., and Olson, E. N. (1998) *Cell* **93,** 215–228
6. Antos, C. L., McKinsey, T. A., Frey, N., Kutschke, W., McAnally, J., Shelton, J. M., Richardson, J. A., Hill, J. A., and Olson, E. N. (2002) *Proc. Natl. Acad. Sci. U. S. A.* **99,** 907–912
7. Bueno, O. F., Wilkins, B. J., Tymitz, K. M., Glascock, B. J., Kimball, T. F., Lorenz, J. N., and Molkentin, J. D. (2002) *Proc. Natl. Acad. Sci. U. S. A.* **99,** 4586–4591
8. De Windt, L. J., Lim, H. W., Bueno, O. F., Liang, Q., Delling, U., Braz, J. C., Glascock, B. J., Kimball, T. F., del Monte, F., Hajjar, R. J., and Molkentin, J. D. (2001) *Proc. Natl. Acad. Sci. U. S. A.* **98,** 3322–3327
9. Hill, J. A., Rothermel, B., Yoo, K. D., Cabuay, B., Demetroulis, E., Weiss, R. M., Kutschke, W., Bassel-Duby, R., and Williams, R. S. (2002) *J. Biol. Chem.* **277,** 10251–10255
10. Rothermel, B. A., McKinsey, T. A., Vega, R. B., Nicol, R. L., Mammen, P., Yang, J., Antos, C. L., Shelton, J. M., Bassel-Duby, R., Olson, E. N., and Williams, R. S. (2001) *Proc. Natl. Acad. Sci. U. S. A.* **98,** 3328–3333
11. Zou, Y., Hiroi, Y., Uozumi, H., Takimoto, E., Toko, H., Zhu, W., Kudoh, S., Mizukami, M., Shimoyama, M., Shibasaki, F., Nagai, R., Yazaki, Y., and Komuro, I. (2001) *Circulation* **104,** 97–101
12. Van Rooij, E., Doevendans, P. A., Crijns, H. J., Heeneman, S., Lips, D. J., Van Bilsen, M., Williams, R. S., Olson, E. N., Bassel-Duby, R., Rothermel, B. A., and De Windt, L. J. (2004) *Circ. Res.* 94, e18–e26
13. Rao, A., Luo, C., and Hogan, P. G. (1997) *Annu. Rev. Immunol.* **15,** 707–747
14. van Rooij, E., Doevendans, P. A., de Theije, C. C., Babiker, F. A., Molkentin, J. D., and de Windt, L. J. (2002) *J. Biol. Chem.* **277,** 48617–48626
15. Wilkins, B. J., De Windt, L. J., Bueno, O. F., Braz, J. C., Glascock, B. J., Kimball, T. F., and Molkentin, J. D. (2002) *Mol. Cell. Biol.* **22,** 7603–7613
16. Pu, W. T., Ma, Q., and Izumo, S. (2003) *Circ. Res.* **92,** 725–731
17. Ranger, A. M., Oukka, M., Rengarajan, J., and Glimcher, L. H. (1998) *Immunity* **9,** 627–635
18. Rockman, H. A., Ross, R. S., Harris, A. N., Knowlton, K. U., Steinhelper, M. E., Field, L. J., Ross, J., Jr., and Chien, K. R. (1991) *Proc. Natl. Acad. Sci. U. S. A.* **88,** 8277–8281
19. van Empel, V. P., Bertrand, A. T., van Oort, R. J., van der Nagel, R., Engelen, M., van Rijen, H. V., Doevendans, P. A., Crijns, H. J., Ackerman, S. L., Sluiter, W., and De Windt, L. J. (2006) *J. Am. Coll. Cardiol.* **48,** 824–832
20. van Oort, R. J., van Rooij, E., Bourajjaj, M., Schimmel, J., Jansen, M. A., van der Nagel, R., Doevendans, P. A., Schneider, M. D., van Echteld, C. J., and De Windt, L. J. (2006) *Circulation* **114,** 298–308
21. Buitrago, M., Lorenz, K., Maass, A. H., Oberdorf-Maass, S., Keller, U., Schmitteckert, E. M., Ivashchenko, Y., Lohse, M. J., and Engelhardt, S. (2005) *Nat. Med.* **11,** 837–844
22. Chuvpilo, S., Avots, A., Berberich-Siebelt, F., Glockner, J., Fischer, C., Kerstan, A., Escher, C., Inashkina, I., Hlubek, F., Jankevics, E., Brabletz, T., and Serfling, E. (1999) *J. Immunol.* **162,** 7294–7301
23. Hoey, T., Sun, Y. L., Williamson, K., and Xu, X. (1995) *Immunity* **2,** 461–472
24. Imamura, R., Masuda, E. S., Naito, Y., Imai, S., Fujino, T., Takano, T., Arai, K., and Arai, N. (1998) *J. Immunol.* **161,** 3455–3463
25. De Windt, L. J., Lim, H. W., Taigen, T., Wencker, D., Condorelli, G., Dorn, G. W., II, Kitsis, R. N., and Molkentin, J. D. (2000) *Circ. Res.* **86,** 255–263
26. Ranger, A. M., Gerstenfeld, L. C., Wang, J., Kon, T., Bae, H., Gravallese, E. M., Glimcher, M. J., and Glimcher, L. H. (2000) *J. Exp. Med.* **191,** 9–22
27. Zaichuk, T. A., Shroff, E. H., Emmanuel, R., Filleur, S., Nelius, T., and Volpert, O. V. (2004) *J. Exp. Med.* **199,** 1513–1522
28. Asagiri, M., Sato, K., Usami, T., Ochi, S., Nishina, H., Yoshida, H., Morita, I., Wagner, E. F., Mak, T. W., Serfling, E., and Takayanagi, H. (2005) *J. Exp. Med.* **202,** 1261–1269
29. Sadoshima, J., and Izumo, S. (1997) *Annu. Rev. Physiol.* **59,** 551–571
30. Esposito, G., Rapacciuolo, A., Naga Prasad, S. V., Takaoka, H., Thomas, S. A., Koch, W. J., and Rockman, H. A. (2002) *Circulation* **105,** 85–92
31. Perrino, C., Naga Prasad, S. V., Mao, L., Noma, T., Yan, Z., Kim, H. S., Smithies, O., and Rockman, H. A. (2006) *J. Clin. Investig.* **116,** 1547–1560
32. Mathew, J., Sleight, P., Lonn, E., Johnstone, D., Pogue, J., Yi, Q., Bosch, J., Sussex, B., Probstfield, J., and Yusuf, S. (2001) *Circulation* **104,** 1615–1621
33. Lowes, B. D., Gilbert, E. M., Abraham, W. T., Minobe, W. A., Larrabee, P., Ferguson, D., Wolfel, E. E., Lindenfeld, J., Tsvetkova, T., Robertson, A. D., Quaife, R. A., and Bristow, M. R. (2002) *N. Engl. J. Med.* **346,** 1357–1365
34. Wilkins, B. J., Dai, Y. S., Bueno, O. F., Parsons, S. A., Xu, J., Plank, D. M., Jones, F., Kimball, T. R., and Molkentin, J. D. (2004) *Circ. Res.* **94,** 110–118